Experimental generation of optical coherence lattices

Yahong Chen, Sergey A. Ponomarenko, and Yangjian Cai

Citation: Applied Physics Letters **109**, 061107 (2016); doi: 10.1063/1.4960966
View online: http://dx.doi.org/10.1063/1.4960966
View Table of Contents: http://scitation.aip.org/content/aip/journal/apl/109/6?ver=pdfcov
Published by the AIP Publishing

Experimental generation of optical coherence lattices

Yahong Chen,[1,2] Sergey A. Ponomarenko,[3,a)] and Yangjian Cai[1,2,a)]
[1]*College of Physics, Optoelectronics and Energy and Collaborative Innovation Center of Suzhou Nano Science and Technology, Soochow University, Suzhou 215006, China*
[2]*Key Lab of Advanced Optical Manufacturing Technologies of Jiangsu Province and Key Lab of Modern Optical Technologies of Education Ministry of China, Soochow University, Suzhou 215006, China*
[3]*Department of Electrical and Computer Engineering, Dalhousie University, Halifax, Nova Scotia B3J 2X4, Canada*

(Received 7 July 2016; accepted 29 July 2016; published online 10 August 2016)

We report experimental generation and measurement of recently introduced optical coherence lattices. The presented optical coherence lattice realization technique hinges on a superposition of mutually uncorrelated partially coherent Schell-model beams with tailored coherence properties. We show theoretically that information can be encoded into and, in principle, recovered from the lattice degree of coherence. Our results can find applications to image transmission and optical encryption. *Published by AIP Publishing*. [http://dx.doi.org/10.1063/1.4960966]

Coherence is one of the fundamental characteristics of a light beam and has played an important role in understanding and tailoring light-matter interactions.[1,2] There is then a small wonder that engineering light coherence properties has received much attention to date motivated by such diverse applications as high-resolution imaging, coherence holography, optical trapping, optical free-space communications, soliton intensity and polarization engineering, and second-harmonic generation.[3–11] Further, recently developed representations of partially coherent light sources, including Gori's non-negative definiteness criterion,[12,13] independent elementary source decomposition,[14] and complex Gaussian representation,[15] have led to the discovery and examination of a plethora of partially coherent beams generated by such sources. Some of the discovered beams with appropriately engineered spatial coherence exhibit nontrivial propagation features such as self-splitting, self-focusing, and self-shaping effects as well as periodicity reciprocity.[16–21] Experimental methods for generation of partially coherent beams with different kinds of correlation functions have been lately advanced.[22–24]

On the other hand, it is well-known that optical lattices have important applications in laser cooling and trapping of neutral atoms, lattice light-sheet microscopy, sorting microscopic particles, and photonic crystals engineering.[25–28] Various kinds of optical lattices including periodic intensity, polarization, and phase distribution have been recently theoretically predicted and experimentally realized.[29–32] Lately, an altogether different kind of optical lattice, optical coherence lattices which refer to the sources having periodic coherence properties, has been theoretically introduced[33] and its free-space propagation properties have been examined in detail.[21] It was found that the coherence lattices may have promising applications to robust free-space optical communications. However, no experimental results relating to optical coherence lattice generation have been reported in the literature. In this letter, we propose and experimentally demonstrate a method to generate coherence lattices through the synthesis of multiple partially coherent Schell-model (PCSM) beams. We also experimentally determine the lobe distribution of generated coherence lattices. Furthermore, we show that optical coherence lattices can carry information which can be recovered through measuring their degree of coherence.

We start by considering a generic partially coherent Schell-model (PCSM) beam with the cross-spectral density expressed as[2]

$$W(\mathbf{r}_1,\mathbf{r}_2)=\sqrt{I(\mathbf{r}_1)I(\mathbf{r}_2)}\mu(\mathbf{r}_1-\mathbf{r}_2), \tag{1}$$

where $I(\mathbf{r})$ is the intensity distribution at the point $\mathbf{r}$. $\mu(\mathbf{r}_1-\mathbf{r}_2)$ is the complex degree of coherence which can be written as

$$\mu(\mathbf{r}_1-\mathbf{r}_2)=|\mu(\mathbf{r}_d)|\exp(i\varphi), \tag{2}$$

where $\mathbf{r}_d=\mathbf{r}_1-\mathbf{r}_2$ and φ is its phase profile.

We consider a generic superposition of multiple Schell-model beams with the cross-spectral density

$$W_s(\mathbf{r}_1,\mathbf{r}_2)=\sum_{m=1}^{M}\sqrt{I^{(m)}(\mathbf{r}_1)I^{(m)}(\mathbf{r}_2)}\left|\mu^{(m)}(\mathbf{r}_d)\right|\exp(i\varphi_m), \tag{3}$$

and the corresponding degree of coherence given by

$$\mu_s(\mathbf{r}_1-\mathbf{r}_2)=\frac{\sum_{m=1}^{M}\sqrt{I^{(m)}(\mathbf{r}_1)I^{(m)}(\mathbf{r}_2)}\left|\mu^{(m)}(\mathbf{r}_d)\right|\exp(i\varphi_m)}{\sum_{m=1}^{M}\sqrt{I^{(m)}(\mathbf{r}_1)I^{(m)}(\mathbf{r}_2)}}. \tag{4}$$

In Eqs. (3) and (4), M is a number of Schell-model beams and $I^{(m)}(\mathbf{r})$ and $\mu^{(m)}(\mathbf{r}_d)$ are the intensity and degree of coherence distributions of the mth PCSM beam, respectively.

Hereafter, we restrict ourselves to a particular case of M identically distributed in intensity Schell-model constituents such that the compound beam degree of coherence can be simplified as

[a)]Authors to whom correspondence should be addressed. Electronic addresses: serpo@dal.ca and yangjiancai@suda.edu.cn.

$$\mu_s(\mathbf{r}_1 - \mathbf{r}_2) = \frac{1}{M}\sum_{m=1}^{M}\left|\mu^{(m)}(\mathbf{r}_d)\right|\exp(i\varphi_m). \tag{5}$$

The degree of coherence can be expressed as[12]

$$\mu_s(\mathbf{r}_1 - \mathbf{r}_2) = \int p_s(\mathbf{v})\exp(i\mathbf{r}_d \cdot \mathbf{v})d\mathbf{v}, \tag{6}$$

where $p_s(\mathbf{v})$ is a non-negative function. Here, $p_s(\mathbf{v})$ is a superposition of M different $p^{(m)}(\mathbf{v})$

$$p_s(\mathbf{v}) = \frac{1}{M}\sum_{m=1}^{M} p^{(m)}(\mathbf{v}). \tag{7}$$

Consider now $p^{(m)}(\mathbf{v})$ in the form

$$p^{(m)}(\mathbf{v}) = \mathrm{circ}\left(\frac{\mathbf{v} - \mathbf{V}_{0m}}{a}\right), \tag{8}$$

where $\mathbf{V}_{0m} = (\mathbf{V}_{0xm}, \mathbf{V}_{0ym})$ and a are the off-axis displacements and the radius of the circle functions.

Substituting from Eqs. (7) and (8) into Eq. (6), we obtain the expression for the compound beam degree of coherence as

$$\mu_s(\mathbf{r}_1 - \mathbf{r}_2) = \frac{1}{M}\sum_{m=1}^{M}\left|\frac{2J_1(a\mathbf{r}_d)}{a\mathbf{r}_d}\right|\exp(i\mathbf{V}_{0m} \cdot \mathbf{r}_d). \tag{9}$$

In Fig. 1, we present density plots of $p_s(\mathbf{v})$ and the lattice degree of coherence magnitude for different M and $\mathbf{V}_{0m}$. In our calculations, we took the radius $a = 0.1$ mm and assumed the adjacent circles to be equidistant with the separation $d = 10$ mm. We can infer from Fig. 1 that the generated beam coherence distribution gradually becomes lattices-like and progresses in its complexity as the magnitude of M increases.

It can be seen in Fig. 1 that $\mu_s(\mathbf{r}_1 - \mathbf{r}_2)$ and $p_s(\mathbf{v})$ are related. Specifically, if $p_s(\mathbf{v})$ is regarded as an image, then $\mu_s(\mathbf{r}_1 - \mathbf{r}_2)$ contains information about the image. This information can be recovered by measuring the lattice degree of coherence. Figure 2 illustrates recovering the information concealed in optical coherence lattices. As shown in Fig. 2(a), $p_s(\mathbf{v})$ is composed of seven circle functions which make up an image "H," and the corresponding lattice degree of coherence magnitude and phase are shown in Figs. 2(b) and 2(c), respectively. Using the relation between $\mu_s(\mathbf{r}_1 - \mathbf{r}_2)$ and $p_s(\mathbf{v})$, (i.e., $p_s(\mathbf{v}) = F[\mu_s(\mathbf{r}_1 - \mathbf{r}_2)]$, where F is the Fourier transform), the concealed image can be recovered from the fast Fourier transform (FFT) of the lattice degree of coherence (see Fig. 2(d)).

We carried out experiments to confirm our numerical results. Our experimental setup for hiding image in the coherence lattices and measurement of coherence lattices is depicted in Fig. 3. A fully coherent He-Ne laser beam of wavelength $\lambda = 632.8$ nm is spatially filtered and collimated by a spatial filter assembly (SF) and a thin lens L_1 with the focal length $f_1 = 100$ mm. The collimated beam then goes to an amplitude mask (AM) which is used to modulate the intensity distribution of the fully coherent collimated beam. The shaped coherent beam from the AM illuminates a rotating ground glass disc (RGGD) producing an incoherent beam whose intensity distribution is the same as that of the shaped coherent beam. It should be noted that the output beam from the RGGD can be regarded as incoherent provided the diameter of the beam spot on the RGGD is much greater than the inhomogeneity scale of the RGGD[1] which is satisfied in our experiment. The motion controller (MC) is used to control the rotating speed of the RGGD which is set to 3000 r/min in our experiment. The output beam from the RGGD is collimated by a lens L_2 with the focal length $f_2 = 250$ mm onto a CCD camera. The complex degree of coherence of the beam detected by the camera can be expressed as

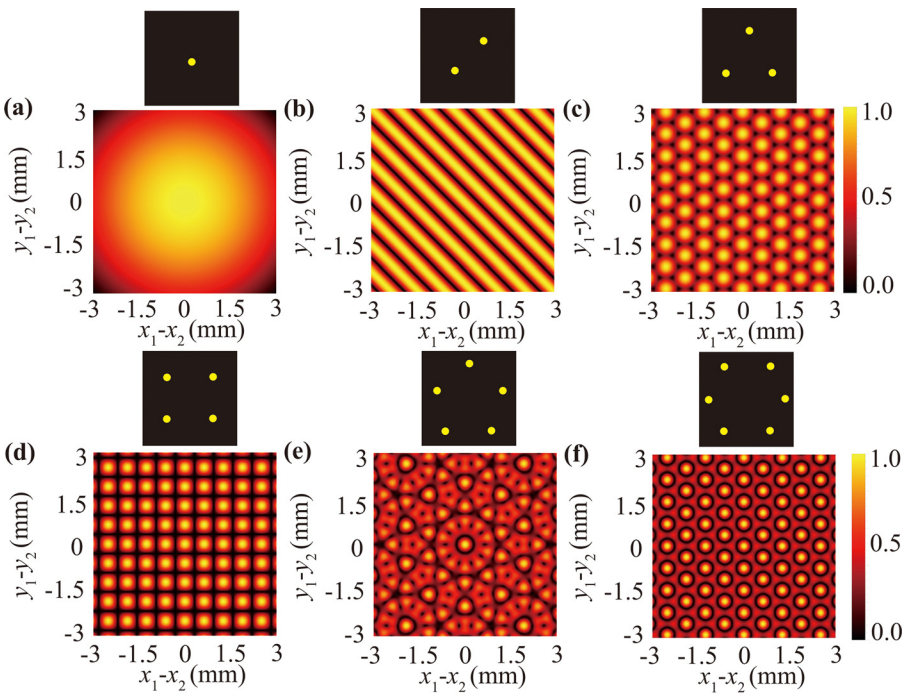

FIG. 1. Density plot of the lattice degree of coherence magnitude distribution and the corresponding $p_s(\mathbf{v})$ distribution (yellow circles on black background) with different M and $\mathbf{V}_{0m}$. (a) $M = 1$; (b) $M = 2$; (c) $M = 3$; (d) $M = 4$; (e) $M = 5$; (f) $M = 6$.

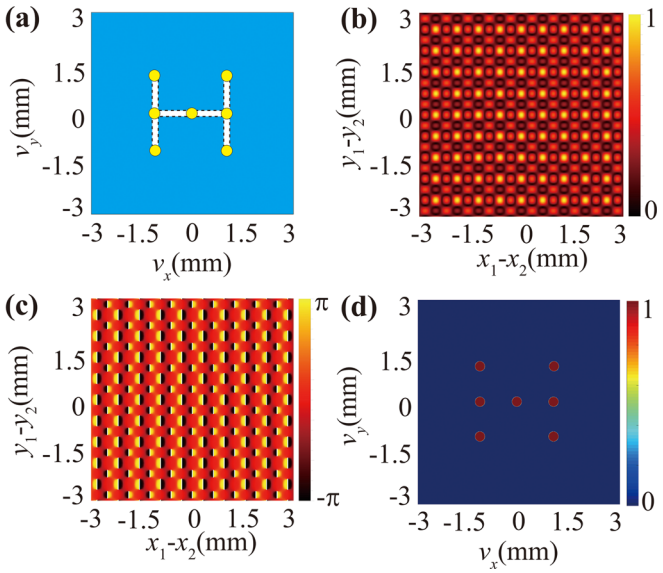

FIG. 2. Recovering information concealed in optical coherence lattices. (a) the image "H" to be hidden; (b) the lattice degree of coherence magnitude distribution of the image; (c) the lattice degree of coherence phase distribution of the image; (d) the recovered image.

$$\mu(\mathbf{r}_d) = \int I(\mathbf{v}) \exp\left(-i\frac{2\pi}{\lambda f_2}\mathbf{r}_d \cdot \mathbf{v}\right) d^2\mathbf{v}, \tag{10}$$

where $I(\mathbf{v})$ is the normalized intensity distribution of the incoherent beam at the RGGD. $I(\mathbf{v})$ is modulated by the amplitude mask (AM), and in our experiment $I(\mathbf{v})$ is a superposition of circle functions such that

$$I(\mathbf{v}) = \frac{1}{M}\sum_{m=1}^{M} I^m(\mathbf{v}) = \frac{1}{M}\sum_{m=1}^{M} \mathrm{circ}\left(\frac{\mathbf{v}-\mathbf{v}_{0m}}{\sigma_0}\right), \tag{11}$$

where σ_0 is the radius of each circle and $\mathbf{v}_{0m}$ are the off-axis displacements of the individual circles. Substituting from Eq. (11) into Eq. (10), we obtain, after integration, the expression for the degree of coherence of the generated partially coherent beam as

$$\mu(\mathbf{r}_d) = \frac{1}{M}\sum_{m=1}^{M} \frac{J_1[2\pi\sigma_0 r_d/(\lambda f_2)]}{\pi\sigma_0 r_d/(\lambda f_2)} \exp\left(-i\frac{2\pi}{\lambda f_2}\mathbf{r}_d \cdot \mathbf{v}_{0m}\right). \tag{12}$$

By comparing Eq. (12) with Eq. (9), we find that the lattice degree of coherence in our experiment has the same form as our theoretical lattice degree of coherence (i.e., Eq. (9)), with the identification $a = \pi\sigma_0/(\lambda f_2)$, $\mathbf{V}_{0m} = -2\pi\mathbf{v}_{0m}/(\lambda f_2)$.

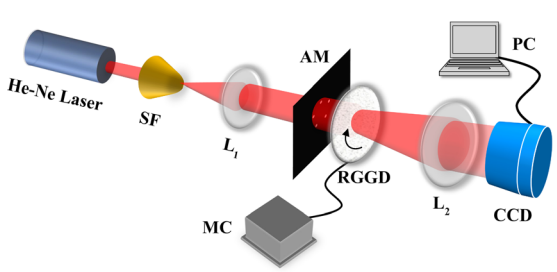

FIG. 3. Experimental setup for generation and measurement of coherence lattices in a partially coherent beam. SF, spatial filter assembly; L_1 and L_2, thin lenses; AM, amplitude mask; RGGD, rotating ground-glass disk; MC, motion controller; CCD, charge-coupled device; PC, personal computer.

Figure 4 shows the intensity distribution of the beam spots with different M at the RGGD, the radius of each circle $\sigma_0 = 0.25$ mm and the adjacent circles are equidistant with the separation $d = 3$ mm. For the case of $M \geq 3$, the beam spots at the RGGD are located at regular polygon vertices. The incoherent beam intensity distributions will lead to linear phase shifts in the complex degree of coherence, giving rise to a lattice structure of the generated beam coherence distribution illustrated in Fig. 5.

In fact, the intensity distribution of the beam spots at the RGGD is the image with information and it is now hidden in the coherence lattices. In order to recover the information of the image, we need to measure the lattice degree of coherence magnitude and phase distribution. We now turn to the experimental determination of the second-order lattice degree of coherence. As shown in Fig. 3, a generated optical coherence lattice arrives at the CCD camera which records an instantaneous intensity of the lattice. Thus, the instantaneous intensity correlations can be inferred using a PC. Such intensity-intensity correlations determine the normalized fourth-order correlation function of the lattice, defined as

$$g^{(2)}(\mathbf{r}_1, \mathbf{r}_2) = \frac{\langle I(\mathbf{r}_1, t) I(\mathbf{r}_2, t)\rangle}{\langle I(\mathbf{r}_1, t)\rangle \langle I(\mathbf{r}_2, t)\rangle}, \tag{13}$$

here $I(\mathbf{r}, t)$ denotes the instantaneous intensity at point $\mathbf{r}$, and $\langle\,\rangle$ denotes the ensemble average. According to the Gaussian moment theorem,[1] the fourth-order correlation function can be expanded in terms of the complex degree of coherence as

$$g^{(2)}(\mathbf{r}_1, \mathbf{r}_2) = 1 + |\mu(\mathbf{r}_1, \mathbf{r}_2)|^2. \tag{14}$$

In our experiment, the integration time of the CCD is 20 ms and the frame rate is 30 FPS. The CCD records 3000 pictures in total, and each picture denotes the realization of the beam cross section. Each realization can be represented by a matrix $I^{(n)}(x, y)$ with x and y being pixel spatial coordinates. Here, n denotes each realization and ranges from 1 to 3000. The degree of coherence magnitude is then obtained as

$$|\mu(\mathbf{r}_1, \mathbf{r}_2 = 0)| = \left(\frac{1}{N}\frac{\sum_{n=1}^{N} I^{(n)}(x, y) I^{(n)}(0, 0)}{\bar{I}(x, y)\bar{I}(0, 0)} - 1\right)^{1/2}, \tag{15}$$

where

$$\bar{I}(x, y) = \sum_{n=1}^{N} I^{(n)}(x, y)/N \quad \text{and} \quad \bar{I}(0, 0) = \sum_{n=1}^{N} I^{(n)}(0, 0)/N, \tag{16}$$

here, $\bar{I}(x, y)$ and $\bar{I}(0, 0)$ denote the average intensity of all realizations and the average intensity at the central point, respectively.

Figure 5 shows the experimental results for the lattice degree of coherence distribution for different M. The experimental results in Fig. 5 clearly show that the degree of coherence distribution becomes lattice-like and it progressively increases in complexity as M increases.

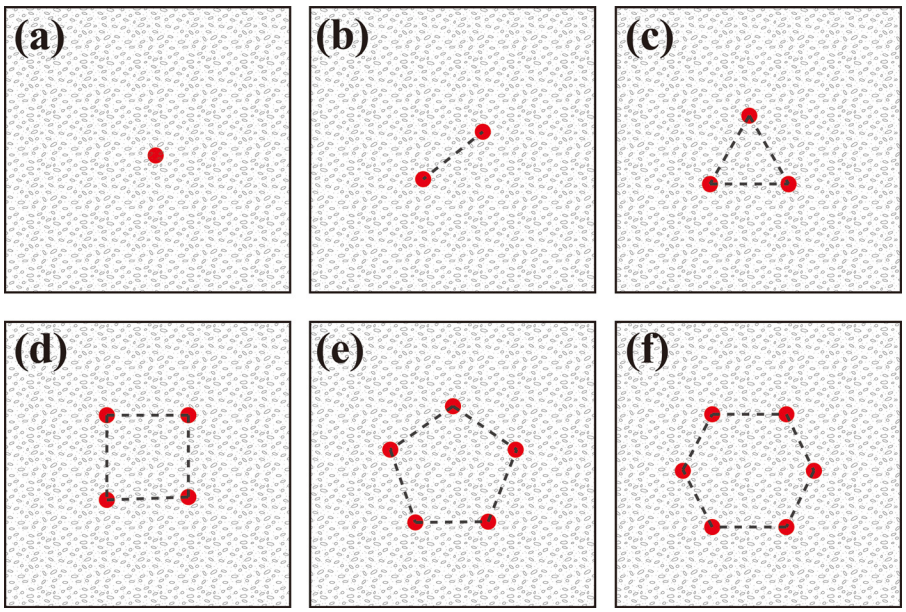

FIG. 4. Intensity distribution of beam spots with different M at the RGGD. (a) $M=1$, (b) $M=2$, (c) $M=3$, (d) $M=4$, (e) $M=5$, and (f) $M=6$.

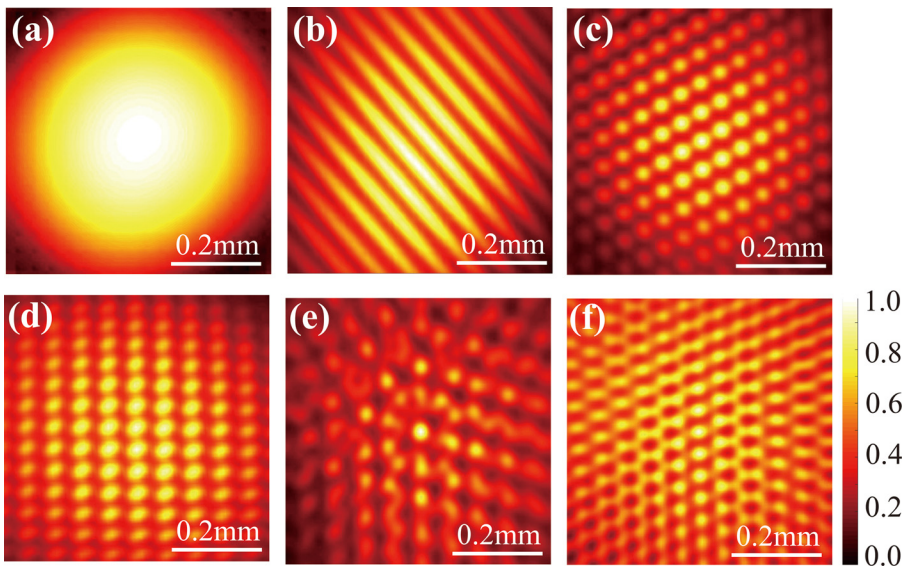

FIG. 5. Experimental results of the lattice degree of coherence magnitude distribution for different M. (a) $M=1$, (b) $M=2$, (c) $M=3$, (d) $M=4$, (e) $M=5$, and (f) $M=6$.

In summary, we have presented a method for generating recently introduced optical coherence lattices. Our approach makes use of a synthesis of multiple partially coherent Schell-model beams. We have discussed that the feasibility of the optical coherence lattices can carry information and we have studied that the information can be recovered from the distribution of lattices degree of coherence. We have also experimentally realized the information hidden in the coherence lattices and determined the degree of coherence of the generated lattices. Our method furnishes a simple and efficient experimental technique to produce optical coherence lattices carrying information, which will be useful in image transmission, robust free-space optical communications, and optical encryption.

This work was supported by the National Natural Science Fund for Distinguished Young Scholar (11525418), the National Natural Science Foundation of China (11274005), the Project of Priority Academic Program Development (PAPD) of Jiangsu Higher Education Institutions, and the National Science and Engineering Research Council of Canada (NSERC).

[1]L. Mandel and E. Wolf, *Optical Coherence and Quantum Optics* (Cambridge University Press, New York, 1995).
[2]E. Wolf, *Introduction to the Theory of Coherence and Polarization of Light* (Cambridge University Press, Cambridge, 2007).
[3]F. Dubois, L. Joannes, and J.-C. Legros, Appl. Opt. **38**, 7085 (1999).
[4]J. N. Clark, X. Huang, R. Harder, and I. K. Robinson, Nat. Commun. **3**, 993 (2012).
[5]M. Takeda, W. Wang, Z. Duan, and Y. Miyamoto, Opt. Express **13**, 9629 (2005).
[6]J. M. Aunón and M. Nieto-Vesperinas, Opt. Lett. **38**, 2869 (2013).
[7]J. C. Ricklin and F. M. Davidson, J. Opt. Soc. Am. A **19**, 1794 (2002).
[8]S. A. Ponomarenko, Phys. Rev. E **64**, 036618 (2001).
[9]S. A. Ponomarenko, Phys. Rev. E **65**, 055601(R) (2002).
[10]S. A. Ponomarenko and G. P. Agrawal, Phys. Rev. E **69**, 036604 (2004).
[11]Y. Cai and U. Peschel, Opt. Express **15**, 15480 (2007).
[12]F. Gori and M. Santarsiero, Opt. Lett. **32**, 3531 (2007).
[13]F. Gori, V. Ramírez-Sánchez, M. Santarsiero, and T. Shirai, J. Opt. A: Pure Appl. Opt. **11**, 085706 (2009).
[14]P. Vahimaa and J. Turiunen, Opt. Express **14**, 1376 (2006).
[15]S. A. Ponomarenko, Opt. Express **19**, 17086 (2011).
[16]S. Sahin and O. Korotkova, Opt. Lett. **37**, 2970 (2012).

[17]H. Lajunen and T. Saastamoinen, Opt. Lett. **36**, 4104 (2011).
[18]Y. Chen, F. Wang, L. Liu, C. Zhao, Y. Cai, and O. Korotkova, Phys. Rev. A **89**, 013801 (2014).
[19]C. Liang, F. Wang, X. Liu, Y. Cai, and O. Korotkova, Opt. Lett. **39**, 769 (2014).
[20]Y. Chen, J. Gu, F. Wang, and Y. Cai, Phys. Rev. A **91**, 013823 (2015).
[21]L. Ma and S. A. Ponomarenko, Opt. Express **23**, 1848 (2015).
[22]F. Wang, X. Liu, Y. Yuan, and Y. Cai, Opt. Lett. **38**, 1814 (2013).
[23]Y. Cai, Y. Chen, and F. Wang, J. Opt. Soc. Am. A **31**, 2083 (2014).
[24]Y. Chen, F. Wang, J. Yu, L. Liu, and Y. Cai, Opt. Express **24**, 15232 (2016).
[25]I. Bloch, J. Dalibard, and S. Nascimbene, Nat. Phys. **1**, 23 (2005).
[26]E. Betzig, Opt. Express **13**, 3021 (2005).
[27]B. Chen, W. R. Legant, K. Wang, L. Shao, D. E. Milkie, M. W. Davidson, C. Janetopoulos, X. S. Wu, J. A. Hammer III, Z. Liu, *et al.*, Science **346**, 1257998 (2014).
[28]M. P. MacDonald, G. C. Spalding, and K. Dholakia, Nature **426**, 421 (2003).
[29]P. Senthilkumaran and R. S. Sirohi, Opt. Commun. **105**, 158 (1994).
[30]Z. Chen and K. McCarthy, Opt. Lett. **27**, 2019 (2002).
[31]S. Vyas and P. Senthilkumaran, Appl. Opt. **46**, 2893 (2007).
[32]M. Kumar and J. Joseph, Appl. Phys. Lett. **105**, 051102 (2014).
[33]L. Ma and S. A. Ponomarenko, Opt. Lett. **39**, 6656 (2014).